APPLIED AND ENVIRONMENTAL MICROBIOLOGY, Nov. 2005, p. 7589–7593
0099-2240/05/$08.00+0 doi:10.1128/AEM.71.11.7589–7593.2005

Vol. 71, No. 11

Bactericidal Actions of a Silver Ion Solution on *Escherichia coli*, Studied by Energy-Filtering Transmission Electron Microscopy and Proteomic Analysis

Mikihiro Yamanaka,* Keita Hara, and Jun Kudo

Research Dept. 8, Devices Technology Research Laboratories, Corporate Research and Development Group, Sharp Corporation, 2613-1, Ichinomoto-cho, Tenri, Nara, Japan

Received 20 April 2005/Accepted 11 July 2005

Bactericidal actions of the silver ion on *Escherichia coli* as a model microorganism were studied using energy-filtering transmission electron microscopy (EFTEM), two-dimensional electrophoresis (2-DE), and matrix-assisted laser desorption ionization–time-of-flight mass spectrometry (MALDI-TOF MS). EFTEM observations demonstrated that the silver ion readily infiltrates the interior of *E. coli*, contrary to the early hypothesis that it resides initially in the cell membrane area. Furthermore, 2-DE and MALDI-TOF MS indicated that the expression of a ribosomal subunit protein as well as that of some other enzymes and proteins is affected by the silver ion. The present results demonstrate for the first time that one of the major bactericidal functions of the silver ion is its interaction with the ribosome and the ensuing inhibition in expression of the enzymes and proteins essential to ATP production.

The silver ion is known to have antimicrobial effects, and it is increasingly utilized in electric appliances, such as washing machines. Many papers have been published on its effects, and early authors hypothesized that the silver ion primarily affects the function of membrane-bound enzymes, such as those in the respiratory chain, through binding to thiol groups (1, 4, 7). However, proteomic insight into the detailed mechanism is still lacking. In this paper, bactericidal actions of a silver ion solution on *Escherichia coli* as a model microorganism was studied using energy-filtering transmission electron microscopy (EFTEM), two-dimensional electrophoresis (2-DE), and matrix-assisted laser desorption ionization–time-of-flight mass spectrometry (MALDI-TOF MS).

Experimental details are as follows. An aqueous solution with a silver ion concentration of 900 ppb was electrolytically prepared by applying a current of 12.5 mA for 28 s between two silver plate electrodes installed in water. The residual chlorine content in water was less than 0.2 mg/liter. The silver ion concentration in the obtained solution was measured with a Hitachi Z-5010 polarized Zeeman atomic absorption spectrophotometer. As a reference, a 0-ppb solution was also prepared, without electrolysis.

As a model microorganism, gram-negative *E. coli* NBRC-3972 was used. Ten milliliters of the aqueous suspension with 10^7 to ~10^8 CFU/ml *E. coli* reacted with 90 ml of a silver ion solution for 30 min, 3 h, and 24 h. Viable cells were enumerated on an agar plate containing 1 g/liter glucose, 2.5 g/liter yeast extract, and 5 g/liter tryptone by the colony count method, after incubation at 35°C for 24 h.

For morphological observation and elemental analysis using EFTEM, *E. coli* cells that reacted with the silver ion were first fixed in 2% glutaraldehyde in 0.1 M sodium cacodylate buffer at 4°C. After being washed with 0.1 M cacodylate buffer, the suspension was osmicated in 2% osmium tetroxide at 4°C for 4 h and then dehydrated repeatedly with increased concentrations of ethanol. The fixed cells were embedded in epoxy resin at 60°C for 48 h and sliced into an approximately-50-nm-thick EFTEM specimen by using a Leica EM UC6 ultramicrotome. The specimen was then coated with an amorphous carbon film. It was further positively stained with uranyl acetate and lead citrate for morphological observation.

The electron probe was focused to a full width at half maximum of 0.9 nm for elemental analysis using energy dispersive X-ray spectroscopy (EDX). Since the signal-to-noise ratio was inadequate for elemental mapping, the data were acquired spot by spot with an analysis time of 2,000 s per spot. The beam position was sufficiently stable to the extent that the drift was less than 1 nm during the analysis.

For proteomic analysis using 2-DE and MALDI-TOF MS, the *E. coli* suspensions that reacted with 900-ppb and 0-ppb silver ion solutions for 3 h were used. Both samples were centrifuged at 2,900 × *g* at 4°C for 20 min, and the precipitates were suspended in lysis buffer and disrupted in a microcentrifuge tube immersed in ice with an ultrasonic probe for 30 s. After centrifugation at 1,600 × *g* for 30 min, the supernatants contained soluble hydrophilic proteins. The quantity of the protein sample for analysis was fixed at 0.4 mg/ml by using a Bio-Rad protein assay method.

In the first dimension, the proteins were separated in 11-cm-long immobilized pH gradient (IPG) gels with a nonlinear gradient ranging from pH 3 to 10. The IPG gels were rehydrated with a 185-μl rehydration solution {8 M urea, 50 mM dithiothreitol, 4% 3-[(3-cholamidopropyl)-dimethylammonio]-1-propanesulfonate (CHAPS), 0.2% carrier ampholyte, 0.0002% bromophenol blue} containing the protein samples at 20°C for 12 h. Isoelectric focusing was conducted using a Bio-Rad Protean IEF Cell system, with the maximum voltage at 8,000 V.

* Corresponding author. Mailing address: Research Dept. 8, Devices Technology Research Laboratories, Corporate Research and Development Group, Sharp Corporation, 2613-1, Ichinomoto-cho, Tenri, Nara, Japan. Phone: 81 743 65 2357. Fax: 81 743 65 3441. E-mail: yamanaka.mikihiro@sharp.co.jp.

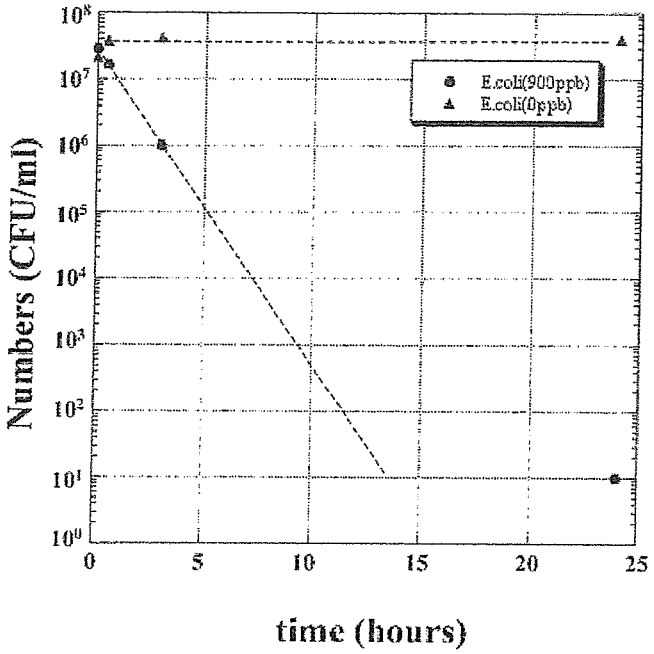

FIG. 1. Viability of *E. coli* cells versus time, as a result of reactions with 900-ppb and 0-ppb silver ion solutions. Viable cells were enumerated on an agar plate containing 1 g/liter glucose, 2.5 g/liter yeast extract, and 5 g/liter tryptone by the colony count method, after incubation at 35°C for 24 h.

After the IPG strips were reconstituted for sodium dodecyl sulfate equilibrium in Bio-Rad Ready Prep equilibration buffers I (6 M urea, 0.375 M Tris-HCl (pH 8.8], 2% sodium dodecyl sulfate, 2% dithiothreitol, 20% glycerol) and II (6 M urea, 0.375 M Tris-HCl [pH 8.8], 2% sodium dodecyl sulfate, 2.5% iodoacetamide, 20% glycerol), 2-DE was carried out with Criterion XT wide gels at 200 V for 30 min. Subsequently, these gels were stained with Sypro Ruby after fixation, and the densitometry profiles were obtained using a Bio-Rad molecular imager (FX Pro). Molecular masses of respective spots were estimated with Bio-Rad PDQuest software, version 7.3. The spots were then cut from the gels with a spot cutter, and the samples for peptide analysis were prepared by the in-gel digestion method. These samples were mixed with a matrix solution (10 mg/ml α-cyano-4-hydroxycinnamic acid in 30% MeCN-0.05% trifluoroacetic acid) and air-dried on a MALDI sample stage. Mass spectra were acquired using an Applied Biosystems Voyager-DE STR instrument in the reflector/delayed extraction mode. The calibration was carried out with the bovine trypsin autodigestion peptide, and the measured peptides were identified using the MS-Fit peptide mass fingerprinting search engine.

Figure 1 shows the viability of *E. coli* cells versus time, as a result of reactions with 900- and 0-ppb silver ion solutions. The reaction with the 900-ppb solution resulted in an exponential decrease in *E. coli* cells with time, from the initial 10^7 CFU/ml to 10^6 CFU/ml in 3 h and further down to 10 CFU/ml in 24 h. In contrast, the decrease was not observed for the 0-ppb solution over 24 h.

Figure 2 shows the zero loss TEM images of the cell structures obtained with elastically transmitted electrons. The cells that reacted with a 0-ppb solution for 24 h showed normal morphology of *E. coli*, with a multilayered surface consisting of the outer membrane, the peptidoglycan layer in periplasmic space, and the cytoplasmic membrane (Fig. 2A and B). Although the corresponding TEM images are not shown, the cells that reacted with a 900-ppb solution for 30 min and 3 h indicated apparently normal morphology, analogous to that shown in Fig. 2A and B, without a discernible degradation in the membrane structures. In contrast, the cells exposed to a 900-ppb solution for 24 h showed various phases in the process of cell death (Fig. 2C and D). In Fig. 2C, which corresponds to an intermediate stage of cell disruption, plasmolysis and partial disappearance of the cytoplasmic membrane are observed. The structure of the outer membrane is apparently unaffected at this stage, and the cell takes on a deformed morphology, with partial lack of the cytoplasmic membrane. In Fig. 2D, which obviously corresponds to the final stage of cell disruption, the outer membrane is progressively lost and the cytoplasm tends to spill out of the cell.

The EDX results (Fig. 3) show that, after a relatively short reaction time of 30 min, silver was already detected in the interior of *E. coli*. This is contrasted to the cell membrane area, where silver was not detected in spite of repeated measurements at different spots. It should be noted that silver is detected in the interior of *E. coli* sometimes, but not always, with sulfur. Osmium and chlorine were detected as artifacts due to specimen preparation. The electron-dense particles in the cytoplasm observed in Fig. 2C are due to condensation of osmium tetroxide used for cell fixation, and they are not silver aggregates. For prolonged reaction times of 3 and 24 h, the amount of accumulated silver estimated from EDX counts scarcely increased (data not shown).

The present observations indicate that bactericidal actions of the silver ion are caused primarily by its interaction with the cytoplasm in the interior of the cell. The silver ion appears to penetrate through ion channels without causing damage to the cell membranes. As discussed later, it denatures the ribosome and suppresses the expression of enzymes and proteins essential to ATP production. These processes seem to render the cell unable to sustain the membrane structures and result in the cell disruption.

This is contrasted to the early hypothesis that the silver ion primarily affects the function of membrane-bound enzymes, such as those in the respiratory chain (1, 4, 7). It should be added that, though the possibility that a very small amount of silver, undetectable by EFTEM, causes damage to the cell membranes prior to affecting the cytoplasm cannot be totally denied, no experimental evidence to that effect was obtained in the present work.

Figure 4 shows the comparison between the analytical Sypro Ruby-stained two-dimensional polyacrylamide gel electrophoresis protein patterns obtained from the suspensions of *E. coli* after reactions with 0-ppb and 900-ppb solutions for 3 h. The reaction for 3 h was selected, considering that, though the silver ion infiltrates the cell interior as early as 30 min and does not significantly increase further, the reaction as short as 30 min is probably insufficient in identifying the differences from unreacted cells, and the reaction much longer than 3 h is inappropriate since most of the cells are already disrupted. Thus, the demonstration of a decreasing trend in the amount

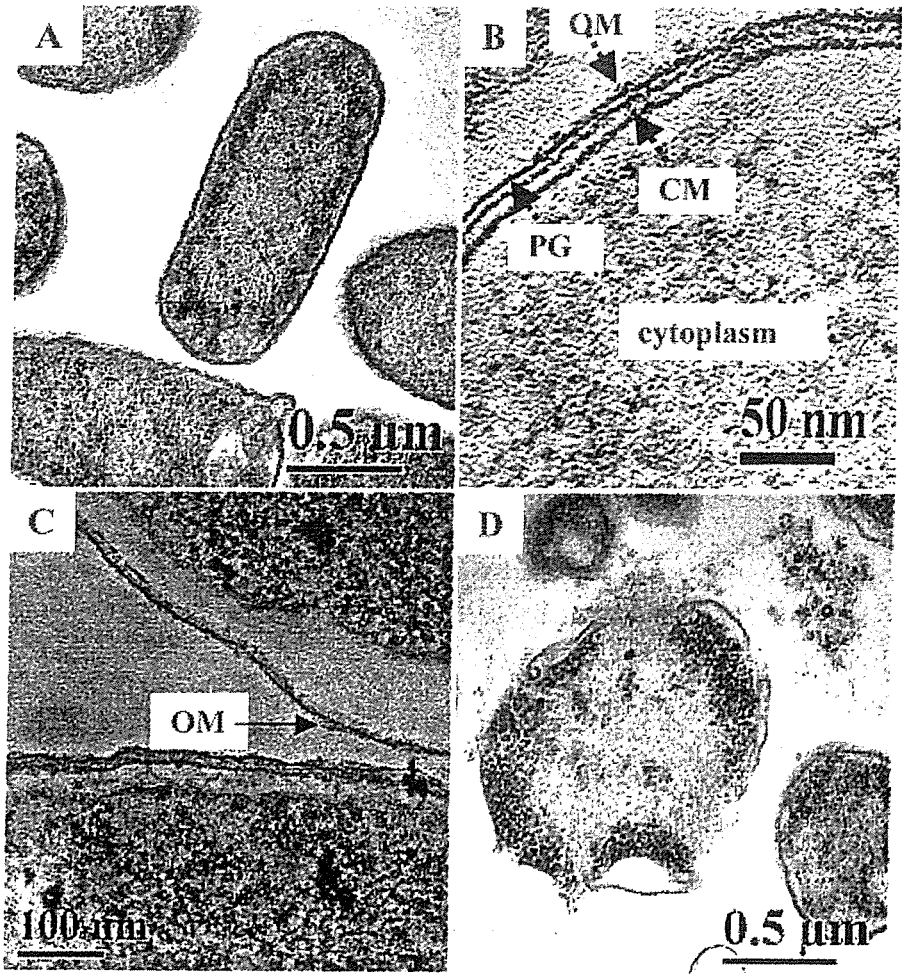

FIG. 2. Zero loss TEM images of an *E. coli* cell. (A) After reaction with a 0-ppb silver ion solution for 24 h. (B) Enlarged view of portion of panel A. (C) After reaction with a 900-ppb silver ion solution for 24 h. (D) Another *E. coli* cell after reaction with a 900-ppb silver ion solution for 24 h. OM, outer membrane; PG, peptidoglycan layer; CM, cytoplasmic membrane.

of protein expression with time, as suggested from the 2-DE patterns, is left for future work.

The 2-DE patterns in Fig. 4 are mutually correlated by two-dimensional gel matching. It should be noted that some spots in the 2-DE patterns indicate a decreased amount of protein expression after reaction with a 900-ppb solution compared to results after reaction with a 0-ppb solution. Four spots with a decrease to less than one-third of the original amount are marked in Fig. 4. These spots were cut from the gels and analyzed using MALDI-TOF MS. Through interrogation of NCBI and Swiss-Prot databases for peptide mass fingerprinting, three proteins, 30S ribosomal subunit protein S2, succinyl-coenzyme A (CoA) synthetase, and maltose transporter (MalK), were identified with high probabilities (Table 1). The other spot, noted as hypothetical, was left unidentified. Fructose-bisphosphate adolase, not shown in Fig. 4, was similarly identified. It is particularly noteworthy that the expression of 30S ribosomal subunit protein S2 was inhibited due to the effect of the silver ion. The ribosome of *E. coli* comprises the 50S and 30S subunits. The 30S subunit contains a 16S RNA plus 20 proteins and plays a crucial role in decoding mRNA by monitoring base pairing between the codon on mRNA and the anticodon on tRNA, while the 50S subunit catalyzes peptide bond formation (8). The present result could be interpreted as follows. The decrease in the expression of the S2 protein due to the effect of the silver ion denatures the ribosome, and its protein- and enzyme-synthesizing function is impaired. Consequently, expression of proteins and enzymes such as maltose transporter, fructose-bisphosphate adolase in the glycolysis pathway, and succinyl-CoA synthetase in the tricarboxylic acid (TCA) cycle is suppressed. It should be noted that, in *E. coli*, succinyl-CoA synthetase catalyzes the intracellular production of ATPs. Furthermore, since the glucose pathway and the TCA cycle play substantial roles towards subsequent production of ATPs in the electron transport chain in the cell membrane area, the inhibition in expression of the enzymes and proteins pertaining to the glucose pathway and the TCA cycle should result in the ultimate deficiency of ATPs, which is indispensable in maintaining cell life. This seems to explain a primary process in bactericidal actions of the silver ion on *E. coli*, which leads to cell death.

In a previous report on bactericidal actions of silver zeolite,

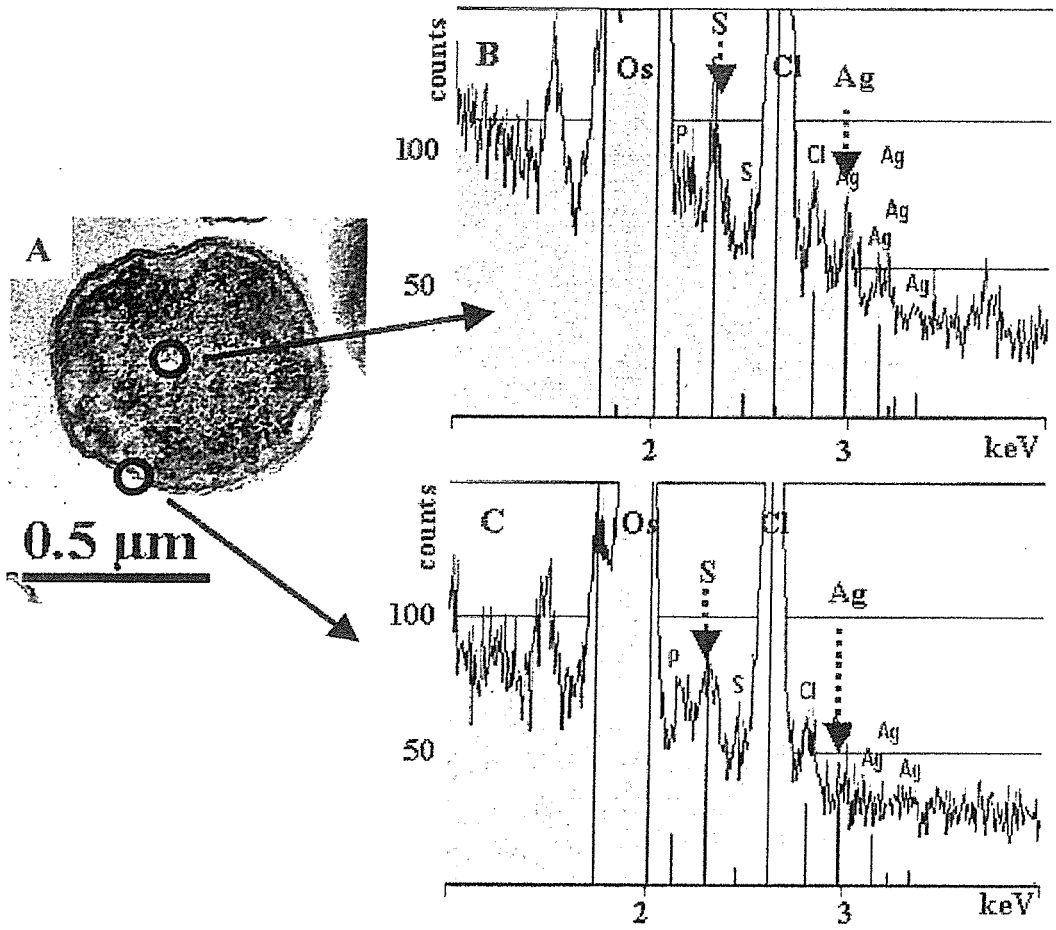

FIG. 3. Scanning TEM (A) and EDX results, indicating that, at a relatively short reaction time of 30 min, silver was already detected in the interior of *E. coli* (B) but not in the cell membrane area (C).

it was hypothesized that two successive processes may be involved (3). First, a bacterial cell in contact with silver zeolite takes in silver ions, which inhibit several functions in the cell and consequently damage it. Second, reactive oxygen species are generated, possibly through the inhibition of a respiratory enzyme(s), and attack the cell. Experimental data indicated that the number of viable *E. coli* cells exposed to a silver zeolite suspension rapidly decreased with time aerobically, while it did not anaerobically. The comparative tests for $AgNO_3$ resulted in a rapid decrease in the number of viable *E. coli* cells under conditions of anaerobiosis as well as aerobiosis.

TABLE 1. Proteins identified through MALDI-TOF MS and interrogation of NCBI and Swiss-Prot databases for peptide mass finger printing

Description	M_r	Accession no. and database	Probability[a]
30S ribosomal subunit protein S2	54.47	26246115; NCBI	69
Succinyl-CoA synthetase	65.69	6980733; NCBI	64
Maltose transporter	88.19	37927753; NCBI	89
Hypothetical protein	80.55	26248233; NCBI	47
Fructose-bisphosphate adolase	36.33	P71295; SwissProt	121

[a] Probabilities were based on the Mowse scoring algorithm.

The first hypothesis in the previous paper (3) is indirectly corroborated by the present observation by EFTEM that the silver ion readily penetrates the interior of the cell. The second hypothesis is not straightforward, since silver is not detected in the cell membrane area where the respiratory chain is located. However, a substantial difference in the bactericidal actions between anaerobiosis and aerobiosis, mentioned above, indicates that aerobiosis prompts bactericidal effects of the silver ion. Previous in vitro analyses of the *E. coli* respiratory chain indicated that reactive oxygen species are generated primarily by the autoxidation of reduced dehydrogenases, such that NADH dehydrogenase II reacted with oxygen at a substantial rate, succinate dehydrogenase produced scant but still detectable reactive oxygen species, and its anaerobically synthesized isozyme, fumarate reductase, was autoxidized rapidly when exposed to air (5). Meanwhile, recent in vivo analyses indicated that reactive oxygen species are primarily formed by a source outside the respiratory chain, and that source has not yet been identified (6). It is noteworthy that the present result confirms that the expression of a ribosomal subunit protein as well as some other enzymes and proteins is inhibited. In particular, the inhibition in the expression of succinyl-CoA synthetase should reduce the catalytic formation of succinate. Since succinate is oxidized to fumarate by the succinate dehydrogenase complex

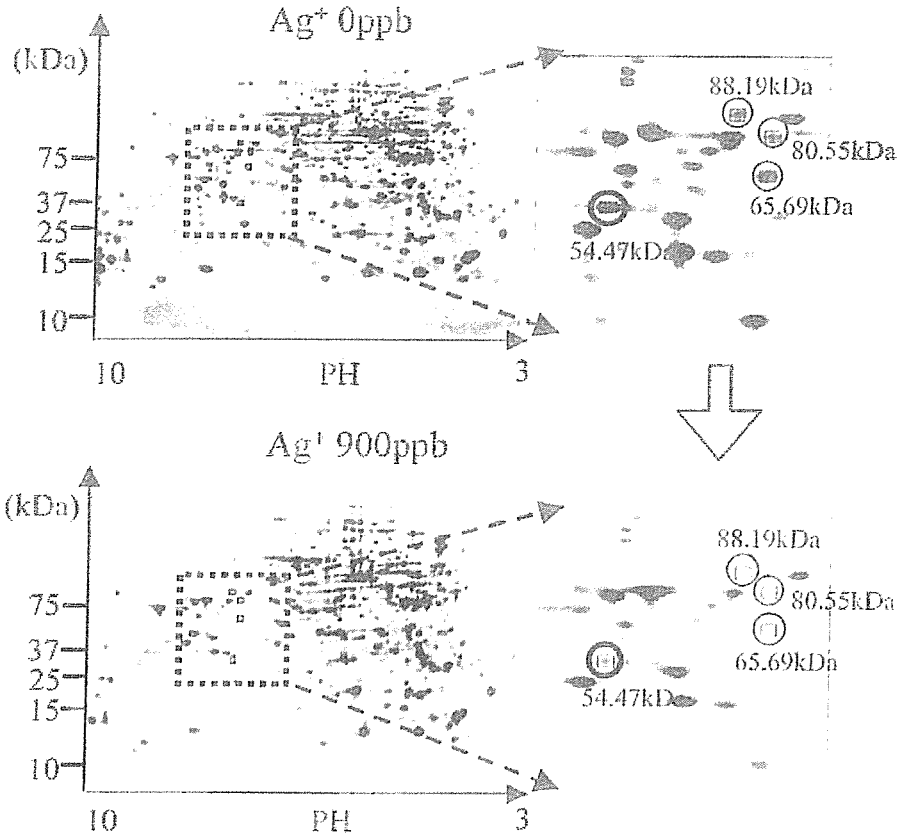

FIG. 4. Analytical Sypro Ruby-stained two-dimensional polyacrylamide gel electrophoresis protein patterns obtained from the suspensions of *E. coli* after reactions with 0-ppb and 900-ppb solutions for 3 h. Some spots indicate decreased amounts of protein expression after reaction with a 900-ppb solution, compared to results after reaction with a 0-ppb solution. Four spots with a decrease to less than one-third of the original amount are marked with open circles.

in the respiratory chain transferring electrons to ubiquinones (2), the inhibition in expression of succinyl-CoA synthetase should exert deleterious effects on the behavior of the respiratory chain through the reduction in electron transfer and generation of ATPs. It may be speculated that the decrease in succinate induces the complementary action of fumarate reductase to convert fumarate to succinate, accompanying the production of reactive oxygen species in the course of the reaction. It is also anticipated that the enzymes involved in the generation of active oxygen species are affected after all in the course of cell death. Further work is certainly necessary to clarify the involvement of oxygen in bactericidal actions of the silver ion on *E. coli* and other microbes.

In conclusion, bactericidal actions of a silver ion solution on *E. coli* were characterized by EFTEM, 2-DE, and MALDI-TOF MS. It was confirmed that the silver ion readily infiltrates the interior of *E. coli*, rather than residing in the cell membrane area, as observed by EFTEM. Subsequent analysis using 2-DE and MALDI-TOF MS indicated that a ribosomal subunit protein and some enzymes and proteins were affected by the silver ion. The present results indicate that one of the major bactericidal actions of the silver ion is caused by its interaction with the ribosome and subsequent suppression in the expression of enzymes and proteins essential to ATP production. The present approach could be extended to other studies related to the silver ion, such as studies of its effects on the viability of microbes with a cell envelope different from that of *E coli*.

We are grateful to Y. Nishikawa (Osaka City University) for fruitful discussions and R. Matsuura (Kyoto-Biseibutu-Kenkyusho) for *E. coli* survival tests. We also thank H. Yoshikawa, M. Ikemizu, and Y. Ikebo for their collaborations and M. Taneya for important advice.

REFERENCES

1. **Bragg, P. D., and D. J. Rainnie.** 1974. The effect of silver ions on the respiratory chains of *Escherichia coli*. Can. J. Microbiol. **20**:883.
2. **Cecchini, G., I. Schroder, R. P. Gunsalus, and E. Maklashina.** 2002. Succinate dehydrogenase and fumarate reductase from *Escherichia coli*. Biochim. Biophys. Acta **1553**:140–157.
3. **Matsumura, Y., K. Yoshikata, S. Kunisaki, and T. Tsuchido.** 2003. Mode of bactericidal action of silver zeolite and its comparison with that of silver nitrate. Appl. Environ. Microbiol. **69**:4278–4281.
4. **McDonnell, G., and A. D. Russell.** 1999. Antiseptics and disinfectants: activity, action, and resistance. Clin. Microbiol. Rev. **12**:147–179.
5. **Messner, K. R., and J. A. Imlay.** 2002. Mechanism of superoxide and hydrogen peroxide formation by fumarate reductase, succinate dehydrongenase, and aspartate oxidase. J. Biol. Chem. **277**:42563–42571.
6. **Seaver, L. C., and J. A. Imalay.** 2004. Are respiratory enzymes the primary sources of intracellular hydrogen peroxide? J. Biol. Chem. **279**:48742–48750.
7. **Uchida, M., T. Yamamoto, and A. Taniguchi.** 2003. Reaction of silver ions and some amino acids. Bokin Bobai **31**:695–704.
8. **Wimberly, B. T., D. E. Brodersen, W. M. Clemons, Jr., R. J. Morgan-Warren, A. P. Carter, C. Vonrhein, T. Hartsch, and V. Ramakrishnan.** 2000. Structure of the 30S ribosomal subunit. Nature **407**:327–339.